Cation ordering in cubic and monoclinic $(Y, Eu)_2O_3$: an x-ray powder diffraction and magnetic susceptibility study

1997 J. Phys.: Condens. Matter 9 365

(http://iopscience.iop.org/0953-8984/9/2/004)

J. Phys.: Condens. Matter **9** (1997) 365–374. Printed in the UK PII: S0953-8984(97)74366-2

Cation ordering in cubic and monoclinic $(Y, Eu)_2O_3$: an x-ray powder diffraction and magnetic susceptibility study

B Antic, M Mitric and D Rodic

'Vinca' Institute of Nuclear Sciences, Laboratory of Solid State Physics, PO Box 522, 11001 Belgrade, Yugoslavia

Received 9 May 1996, in final form 4 July 1996

Abstract. Mixed sesquioxides $Y_{2-x}Eu_xO_3$ ($x = 0.10$, 0.20, 0.60, 1.00, 1.60 and 1.80) in the cubic (C) phase were obtained by precipitation and subsequent sintering. Cubic Eu_2O_3 and $Y_{0.20}Eu_{1.80}O_3$ were transformed into monoclinic (B) phases at 1400 K and 1600 K respectively. The transformation is reconstructive in character. All of the structures were refined using the Rietveld powder method, and the Eu^{3+} ions found to be randomly distributed. The molar magnetic susceptibilities at room temperature exceed the free-ion values, and are almost independent of the concentration for $x \geqslant 0.60$. For $x \leqslant 0.20$, the susceptibilities decrease with decreasing concentration of the magnetic ion Eu^{3+}. This behaviour is attributed to crystal-field and anisotropic exchange effects.

1. Introduction

The mixed sesquioxides $Y_{2-x}Eu_xO_3$ belong to the family of diluted magnetic semiconductors (DMSs) $Y_{2-x}R_xO_3$ (R = magnetic rare-earth ion). These DMSs represent solid solutions where R^{3+} ions replace nonmagnetic Y^{3+} ions in diamagnetic Y_2O_3. Their properties, which depend on the magnetic ion concentration, can be controlled in the process of synthesis.

The starting compounds in the synthesis of the solid solutions $Y_{2-x}Eu_xO_3$ were the sesquioxides Eu_2O_3 and Y_2O_3. At lower temperatures, these oxides crystallize in the space group $Ia3$ of the cubic system, with the C-type structure of bixbyite (Mn_2O_3). In this structure type, cations occupy two nonequivalent special positions 24d (local symmetry C_2) and 8b (local symmetry C_{3i}). The oxygen ions are in the general 48e positions [1]. Details of the structure properties of cubic $Y_{2-x}R_xO_3$ (R = Gd, Dy, Ho) are given in earlier papers [2–4].

The Eu_2O_3 transforms from the cubic to the monoclinic (C $\rightarrow$ B) form at temperatures in the range 1345–1620 K [5]. The B phase is quenchable [5], but on very slow cooling the transition becomes reversible [5, 6]. The pressure–temperature dependence of the phase transition (C $\rightarrow$ B) has also been studied [7]. Monoclinic Y_2O_3 has been obtained under high pressure, and the transformation was found to be reversible [7]. The synthesis of the cubic mixed oxides $Y_{2-x}Eu_xO_3$ and the investigation of their transformation to the monoclinic phase (C $\rightarrow$ B) are among the aims of this paper.

In the bixbyite structure type, rare-earth magnetic ions may replace nonmagnetic ions preferentially or randomly over two cationic sites (8b and 24d). The distribution of Eu^{3+} ions in cubic $Y_{2-x}Eu_xO_3$ was investigated earlier by measuring the magnetic susceptibility [8]. It was found that Eu^{3+} ions preferentially occupy 24d sites [8]. However, another

0953-8984/97/020365+10$19.50

low-temperature magnetic susceptibility study has shown the opposite result, i.e. random distribution [9]. The distribution of magnetic ions is important because it affects both the magnetic and the electric properties of the materials. For that reason we have studied this distribution by an x-ray diffraction method and by measuring the magnetic susceptibility at room temperature.

The Eu^{3+} ($4f^6$) ions have a singlet $^7F_0$ ground state. An important characteristic of Eu^{3+} ions is that the separations between the different energy levels are comparable with k_BT at room temperature. The energy difference between the first higher $^7F_1$ state and the $^7F_0$ ground state of Eu^{3+} in Eu_2O_3 is 250 cm^{-1} [10]. As a consequence, the higher-lying states are populated even below room temperature and they must be taken into consideration when investigating the magnetic properties of Eu^{3+} ions and their compounds. Measurement of the magnetic susceptibility of $Y_{2-x}Eu_xO_3$ at room temperature will help to elucidate the crystallographic distribution and magnetic properties of Eu^{3+} ions in the host Y_2O_3.

2. Experimental details

2.1. Preparation of cubic and monoclinic $Y_{2-x}Eu_xO_3$

The solid solutions of $Y_{2-x}Eu_xO_3$ ($x = 0.10$, 0.20, 0.60, 1.00, 1.60 and 1.80) were made from the cubic sesquioxides Eu_2O_3 (purity 99.985%) and Y_2O_3 (purity 99.99%). The starting oxides were mixed in appropriate molar ratios and dissolved in HNO_3. Precipitation of the hydroxides was achieved by the addition of NH_4OH. The precipitates were washed in distilled water and then dried. The mixtures were pressed into tablets at a pressure of 0.3 GPa and heated at 1250 K for 48 h. The samples were reground, pressed again and heated under the same conditions. X-ray diffraction showed only the cubic phase in all of the samples.

To study the influence of the preparation method on the cationic distribution and other properties we have tried to synthesize the samples with $x = 0.20$ and $x = 0.40$ by direct sintering of homogeneous mixtures of the oxides Eu_2O_3 and Y_2O_3. The mixtures were presintered and sintered at a temperature near that of the structural phase transition of Eu_2O_3 (1320 K). The sample with $x = 0.40$ was not single phase. The x-ray data for the sample with $x = 0.20$ gave strange profiles, approximately triangular, with large FWHMs. In the sample with $x = 0.20$ the reaction between the oxides was incomplete. Both samples were excluded from the following experiments.

$Y_{0.20}Eu_{1.80}O_3$ and Eu_2O_3 samples were obtained in the monoclinic B phase by pressing at 0.3 GPa and heating the corresponding C phases. All of the $Y_{2-x}Eu_xO_3$ and Eu_2O_3 samples were heated at 1400 K for 7 h. Only Eu_2O_3 transformed into the B phase at this temperature. The monoclinic $Y_{0.20}Eu_{1.80}O_3$ was obtained by heating the cubic phase at 1600 K. Heating at 1750 K for 7 h did not produce a C $\rightarrow$ B transformation for samples with $x \leqslant 1.60$.

The C $\rightarrow$ B transformation was recorded using high-temperature diffraction. The cubic $Y_{0.20}Eu_{1.80}O_3$ was heated from 1350 K up to 1650 K, in steps of 20 K, for 30 min and the procedure was recorded using x-ray diffraction on a Philips diffractometer. On heating, reflection from the B phase appeared. However, the transformation was only partial. The pure B phase was obtained after pressing and heating the sample at 1600 K for 7 h. It was found that the C $\rightarrow$ B transition was irreversible, and its temperature was dependent on the heating time and heating temperature.

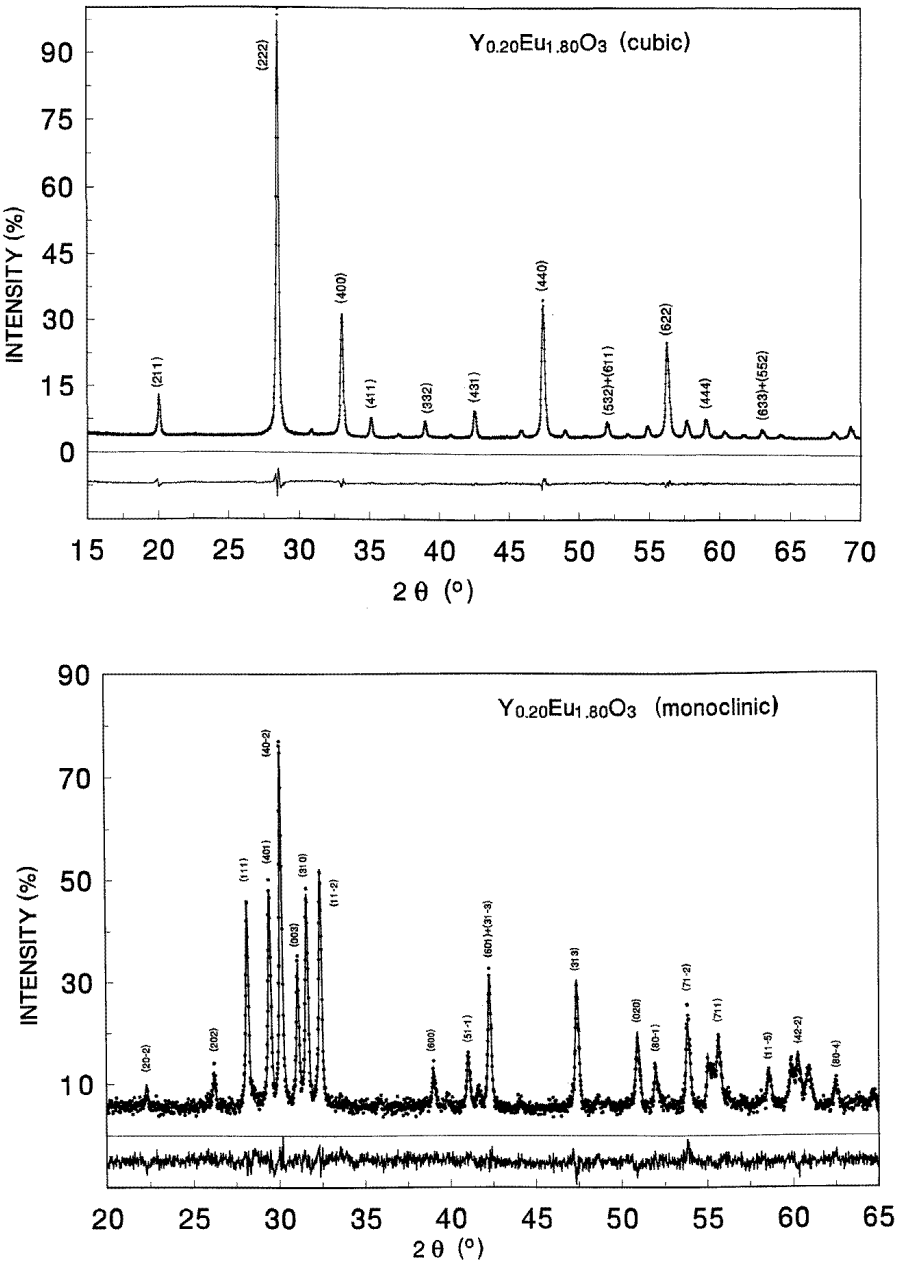

Figure 1. Part of the x-ray diffraction powder pattern of C- and B-$Y_{0.20}Eu_{1.80}O_3$. Dots represent experimental values, the line denotes calculated values, and their differences are given at the bottom of the figures.

2.2. X-ray and magnetic susceptibility measurements

The x-ray data for C-$Y_{2-x}Eu_xO_3$ samples (sintered at 1250 K and further heated at 1400 K) and for B-phase samples were collected on a Philips diffractometer (Cu Kα). The scanning

2θ-range was 10–110° for samples of B phase and 15–115° for C-phase samples. The step was 0.02° and the scanning time was 10 s per step.

The magnetic susceptibility of $Y_{2-x}Eu_xO_3$ was measured at room temperature using the Faraday method. The applied DC field was 0.6 T. The paramagnetic susceptibility was obtained by subtracting the diamagnetic part from the experimental values. The magnetic susceptibility of Y_2O_3 was measured and found to be -24×10^{-6} emu mol^{-1}. This value was used as the diamagnetic contribution for all of the samples.

3. Results and discussion

3.1. Refinement of cubic $Y_{2-x}Eu_xO_3$

The diffraction data for cubic samples of $Y_{2-x}Eu_xO_3$, with concentrations $x = 0.20$, 0.60, 1.00, 1.60, 1.80, were used to refine their crystal structures. The crystal structure refinements were done by the Rietveld profile method assuming the space group $Ia3$ and bixbyite structure type, with the use of the software package DBWS-9411. In the crystal structure refinement, the following atomic and crystal data were refined: lattice parameters (a), occupation numbers (N) (coupled in order to keep the stoichiometric ratio constant), thermal isotropic factors (B) (for three crystallographic positions), and one coordinate for cations in the 24d position and three for oxygen ions in the general position. Eleven parameters describing the background, profile shape, asymmetry, zero point and scale factor were refined.

The peak shape was fitted to the pseudo-Voigt profile function. The ionic scattering curves for Y^{3+} and Eu^{3+} [11] and for O^{2-} [12] were used. The final R-factors (Bragg's, the weighting profile and the profile) were below 10% for all of the samples. Part of the C-$Y_{0.20}Eu_{1.80}O_3$ diffraction pattern is shown in figure 1.

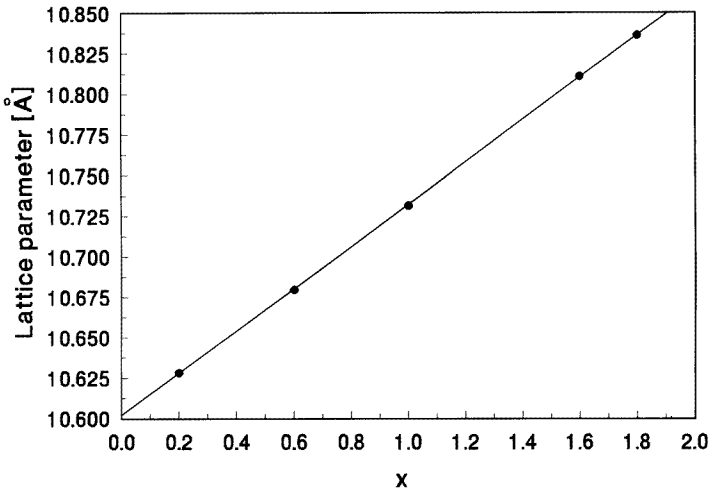

Figure 2. The lattice parameter versus the magnetic ion concentration for C-$Y_{2-x}Eu_xO_3$.

The values of the lattice parameters a, obtained by the crystal structure refinement, are given in figure 2. Vegard's rule was obeyed: $a(x) = a_0 + bx$ with $a_0 = 10.6015(6)$ and $b = 0.1310(5)$. The coefficient b reflects the difference in ionic radii of Eu^{3+} and Y^{3+}. In

the bixbyite type of structure the relationship between lattice parameters and cationic radii is: $\delta r = r(Eu^{3+}) - r(Y^{3+}) = 2b/4 = 0.066$ Å [3]. For comparison, the difference in ionic radii for Eu^{3+} and Y^{3+} coordinated by six anions is $\delta r^* = 0.058$ Å [13].

Table 1. Refined occupation numbers (N), cation–anion distances (d), and isotropic thermal factors (B) for C-$Y_{2-x}Eu_xO_3$.

Concentrations x:	0.20	0.60	1.00	1.60	1.80
$N(\mathrm{Eu})_{8b}$	0.11(2)	0.31(3)	0.52(4)	0.80(3)	0.93(2)
$N(\mathrm{Y})_{8b}$	0.89(2)	0.69(3)	0.48(4)	0.20(3)	0.07(2)
$N(\mathrm{Eu})_{24d}$	0.29(2)	0.89(3)	1.48(4)	2.40(3)	2.67(3)
$N(\mathrm{Y})_{24d}$	2.71(2)	2.11(3)	1.52(4)	0.60(3)	0.33(3)
d_{8b-48e} (Å)	2.287(8)	2.287(9)	2.28(1)	2.33(1)	2.340(7)
$\langle d_{24d-48e}\rangle$ (Å)	2.290(8)	2.30(1)	2.32(1)	2.33(2)	2.333(7)
B_{8b} (Å^2)	0.73(6)	0.7(1)	0.5(1)	0.3(1)	0.61(5)
B_{24d} (Å^2)	0.48(4)	0.47(6)	0.52(6)	0.30(8)	0.36(3)
B_{48e} (Å^2)	1.3(1)	1.0(2)	0.6(2)	0.8(3)	0.7(1)

The values obtained for the occupation numbers N (table 1) show that magnetic ions occupy both cationic sites, 8b and 24d, for all of the samples investigated. The distribution coefficients, $N(\mathrm{Eu})_{24d}N(\mathrm{Y})_{8b}/N(\mathrm{Eu})_{8b}N(\mathrm{Y})_{24d}$, are 1.15, 1.07, 1.11, 1.00 and 1.64 for the corresponding concentrations with increasing x in table 1. Hence, there is no significant partitioning between cationic sites, and the random crystallographic distribution was obtained. Note that in the samples $Y_{2-x}Gd_xO_3$ with a difference in cationic radii, $\delta r^* = r(Gd^{3+}) - r(Y^{3+}) = 0.046$ Å [3], a preferential distribution of the magnetic ions was found [2] and in the samples $Y_{2-x}R_xO_3$ (R = Dy, Ho) with a smaller difference in ionic radii (e.g. $\delta r = r(Dy^{3+}) - r(Y^{3+}) = 0.014(2)$ Å) a random distribution was obtained [3, 4]. On the basis of earlier investigations of the influence of the difference in cationic radii on the distribution [3], partitioning was expected in $Y_{2-x}Eu_xO_3$ samples because the difference in cationic radii is larger than that in $Y_{2-x}Gd_xO_3$. The results obtained can be understood as a consequence of the preparation method affecting the cationic distribution in C-$Y_{2-x}Eu_xO_3$ samples. The samples studied earlier were obtained directly by sintering pure sesquioxides of yttrium and appropriate rare earths [2–4]. The difference between the results of Grill and Schieber [8] and those in this paper can likewise be attributed to the difference in the preparation method. Kern and Kostalecky found that preparation of $Y_{2-x}Eu_xO_3$ by coprecipitation [9] gave the same cationic distribution as in our case.

We shall briefly discuss the cationic first coordination spheres. It is known that the cations in both cationic sites are coordinated by six oxygen ions [1]. The oxygen ions are equidistant for cations in 8b positions (table 1) but the angles deviate from 90°. The polyhedron around the 8b site is a trigonal antiprism. The oxygen ions around 24d sites are distributed in the conformation two + two + two at three distances. The average cation (24d)–anion distances are shown in table 1. The values of the cation–anion distances vary with the magnetic ion concentration, as a consequence of the differences in cationic radii. The variances in bond lengths and angles also change. As a quantitative measure of the distortion we have used a modification of the relation given in [14]:

$$\sigma^2(\theta) = \left(\sum_i (90^\circ - \theta_i)^2\right) \Big/ 8. \tag{1}$$

This relation gives a measure of the degree of distortion from ideal octahedral coordination.

For all of the refined structures the angles and bonds were found. The eight independent angles in the coordination polyhedra around the 24d and 8b sites were used to determine the values $\sigma^2(\theta)$. The values of σ^2 obtained for the 24d site are found to be 453–465°, and those of σ^2 for the 8b site are 23–30° for different samples.

Table 2. Refined crystal and atomic parameters of monoclinic $Y_{0.20}Eu_{1.80}O_3$ (space group $C2/m$). Asterisks denote parameters which did not vary in the last cycle of the refinement (see the text). The corresponding R-factors (profile, weighted profile and Bragg) are given.

Crystal parameters:			
$a = 14.0919(8)$ Å, $b = 3.5891(2)$ Å, $c = 8.7843(5)$ Å			
$\beta = 100.153(3)°$, $\rho = 7.72$ g cm^{-3}, $V = 437.34(2)$ Å^3			
	Atomic parameters		
	x	y	z
Eu1, Y1	0.1318(6)	1/2	0.4998(8)
Eu2, Y2	0.1930(7)	1/2	0.1361(8)
Eu3, Y3	0.4727(9)	1/2	0.178(1)
O1	0.085(2)	0	0.347(3)
O2	0.334(3)	1/2	0.033(3)
O3	0.280(3)	1/2	0.347(4)
O4	0.464(2)	0	0.249(3)
O5	0	1/2	0
$B_{\text{overall}} = 0.91(1)$ Å^2, $N(\text{Eu}i) = 0.9^*$, $N(\text{Y}i) = 0.1^*$			
R-factors:			
R_p (%) = 2.48, R_{wp} (%) = 3.15, R_B (%) = 12.35			

3.2. The refinement of monoclinic B-$Y_{2-x}Eu_xO_3$ ($x = 1.80$, 2.00)

The diffraction data for B-$Y_{2-x}Eu_xO_3$ ($x = 1.80$ and 2.00) were compared with known data for B-Sm_2O_3 [15] and B-Eu_2O_3 [16]. The refinement process on the B-phase samples was done in the space group $C2/m$, using the atomic and crystal parameters of single-crystal B-Eu_2O_3 as starting values [16]. In this space group three kinds of cation occupy 4i positions, four kinds of oxygen ion are in 4i positions and one oxygen ion is in a 2a position [15]. The crystal structure is described in detail by Cromer [15]. In the crystal structure refinement the ionic scattering curves of Y^{3+}, Eu^{3+} and O^{2-} were used. In the last cycle of the refinement of B-$Y_{0.20}Eu_{1.80}O_3$, the 32 parameters were varied: the atomic and crystal parameters (listed in table 2) and the rest were: five background coefficients, five parameters describing the profile shape of the pseudo-Voigt profile function, the zero point, the asymmetry parameter and the scale factor. The refined atomic and crystal parameters for the sample of B-$Y_{0.20}Eu_{1.80}O_3$ are given in table 2, and part of the diffraction pattern is shown in figure 1.

Our powder refinement is about one order of magnitude worse as regards accuracy than a single-crystal refinement of Eu_2O_3 [16]. This is to be expected given the very low signal/background ratio apparent from the powder pattern (figure 1). The unit-cell parameters for single-crystal Eu_2O_3 [16] were: $a = 14.1105(2)$ Å, $b = 3.6021(1)$ Å, $c = 8.8080(2)$ Å, $\beta = 100.037(1)°$, and the powder data obtained by us are: $a = 14.083(9)$ Å, $b = 3.597(2)$ Å, $c = 8.793(6)$ Å, $\beta = 100.070(3)°$. The results are the same within

Table 3. Cation–anion distances in the first coordination spheres for monoclinic $Y_{0.2}Eu_{1.80}O_3$.

Eu1, Y1–O*i*	$d_{\text{cat-an}}$ (Å)	Eu2, Y2–O*i*	$d_{\text{cat-an}}$ (Å)	Eu3, Y3–O*i*	$d_{\text{cat-an}}$ (Å)
2O1	2.27(2)	O3	2.03(3)	2O4	1.19(1)
2O3	2.45(2)	2O2	2.32(2)	O1	1.97(3)
O3	2.67(4)	O2	2.32(4)	O2	2.14(4)
O4	2.78(3)	O5	2.771(9)	2O5	2.455(7)
O4	2.93(3)	2O1	3.16(3)	O3	3.32(5)

the sum of three standard deviations. The three kinds of cation are coordinated by seven oxygen ions. In each case there are five different distances, two pairs of oxygen ions being equidistant. The cation–anion distances are given in table 3.

In order to investigate the cation distribution the cationic occupation numbers were varied in two ways: by refining all three independently, or by refining two coupled occupancies whilst holding the third fixed. The changes in R-factors and in the temperature factors (B) indicate a random distribution of magnetic ions. That is, for a preferential distribution the R-factors become bigger and B_{overall} (correlated with the occupancies) becomes negative. Consequently in the last cycle of the refinement, equal cationic substitution on all sites was assumed and the occupation numbers were not varied. The accuracy of these results is lower than that of those obtained for a more symmetrical cubic phase. Note that the signal/background ratio is bigger for cubic than for monoclinic samples.

3.3. The structural phase transition from the C phase to the B phase

C-Eu_2O_3 and C-$Y_{0.20}Eu_{1.80}O_3$ were transformed irreversibly to the B phase (see section 2). It was found that the apparent temperature of the structural phase transition (C $\rightarrow$ B) depends both on the temperature and on the heating time. This is the reason for the variation in the transition temperatures (1320–1620 K) reported for Eu_2O_3 [5]. It is also known that crystallinity influences the temperature of the structural phase transition [6].

In the crystal phase transition (C $\rightarrow$ B), the cubic form transforms to the monoclinic form with lower symmetry. The space group $C2/m$ is not a subgroup of $Ia3$ and this confirms that the phase transition is of first order [17]. Furthermore, the transformation is kinetically slow and the B phase is quenchable.

In the cubic C phase, cations are coordinated by six oxygen ions, and in the monoclinic B phase, they are coordinated by seven oxygen ions. Since a change in primary coordination occurs, the transition is reconstructive [18].

The C $\rightarrow$ B temperature transformation of $Y_{2-x}Eu_xO_3$ decreases with the magnetic ion concentration. It is possible that at higher temperatures $T > 1750$ K at atmospheric pressure, the same phase transition occurs in $Y_{2-x}Eu_xO_3$ for $x \leqslant 1.80$. For samples with very low concentrations of magnetic ions the phase transition is expected only at high pressures, as in pure Y_2O_3 [7].

3.4. Magnetic properties of Eu^{3+} *ions in* $Y_{2-x}Eu_xO_3$

The magnetic properties of Eu^{3+} ions in $Y_{2-x}Eu_xO_3$ were studied by measuring the magnetic susceptibilities at room temperature for C-phase samples synthesized at two different temperatures, 1400 K and 1600 K, for Eu_2O_3 synthesized at 1250 K, and for B-phase samples. The calculated molar susceptibilities of Eu^{3+} ions at room temperature are shown

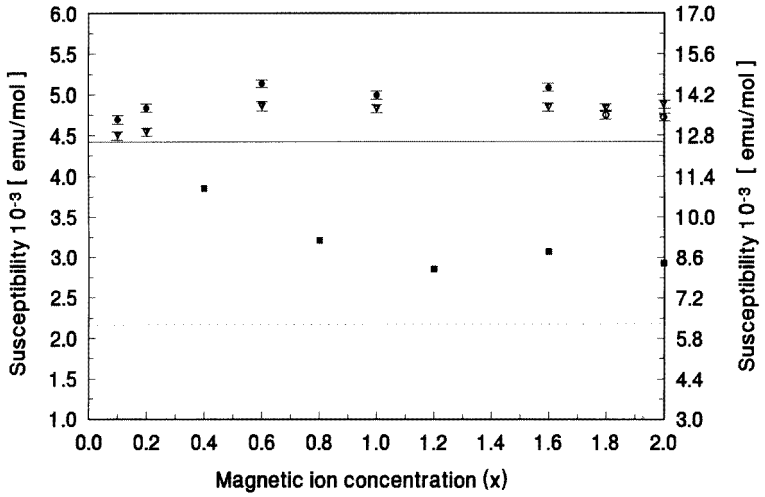

Figure 3. The dependence of the molar susceptibilities of Eu^{3+} in $Y_{2-x}Eu_xO_3$ at room temperature on the magnetic ion concentration, for (▼) samples obtained at 1400 K (except Eu_2O_3), (●) samples with additional firing at 1600 K, and (○) B-phase samples; also (■) results from [8] at 95 K are given for comparison (see the text). Solid and dotted lines represent the calculated values for room temperature and 95 K, respectively (see the text).

in figure 3. It can be seen in figure 3 that the susceptibility behaviours are similar for the B and C phases, and for C-phase samples fired at different temperatures. The molar susceptibility is almost constant for $x \geqslant 0.6$, but decreases for lower x in all cases. The very different data of Grill and Schieber [8] are also shown in figure 3.

The susceptibility of free Eu^{3+} ions was calculated both for room temperature and for 95 K (the solid line and the dotted line in figure 3, respectively), by using Van Vleck's equation [19, 20]:

$$\chi = \left[N\sum_J\left(\frac{g_J^2\mu_B^2 J(J+1)}{3k_BT}+\alpha\right)(2J+1)\exp\left(\frac{-E_J}{k_BT}\right)\right]\Big/\left[\sum_J(2J+1)\exp\left(-\frac{E_J}{k_BT}\right)\right] \tag{2}$$

where E_J denotes the theoretical energy levels of Eu^{3+} given by Judd [21], J is the total angular quantum number, g_J is the Landé splitting factor, μ_B is the Bohr magneton, T is the absolute temperature, k_B denotes the Boltzmann constant, and α is Van Vleck's term, given by [19, 20]

$$\alpha = \frac{\mu_B^2}{6(2J+1)}\left[\frac{F_{J+1}}{E_{J+1}-E_J}-\frac{F_J}{E_J-E_{J-1}}\right] \tag{3}$$

where $F_J = (1/J)[(S+L+1)^2 - J^2][J^2-(S-L)^2]$.

To explain the results given in figure 3, we must consider: (a) the crystal-field effect (CFE), (b) exchange interactions (isotropic and anisotropic), (c) the influence of the preparation method, and (d) the influence of the firing temperature. These effects are discussed below.

The ground state $^7F_0$ is a singlet, and the crystal field has an influence on the splitting of the higher multiplets which are populated at room temperature. Theoretical calculations of the magnetic susceptibility χ show that the higher states $^7F_1$ and $^7F_2$ give important

contributions and states with $J \geqslant 3$ can be neglected. It was found that the crystal field in Eu_2O_3 increases the susceptibility to above the free-ion value [22]. The behaviour obtained for χ per mole (χ_{mol}) versus x must be considered as a consequence of the combined action of a CFE and exchange interactions. Also, it was found that the temperature of preparation may influence the χ_{mol}-values. The samples ($x \leqslant 1.60$) which were fired at 1600 K (●) have values of χ_{mol} different to those for samples fired at 1400 K (▼) (figure 3). This result indicates that the different firing conditions influence the atomic and crystal parameters. As a consequence, the change in crystal-field intensity occurs, and the values of χ_{mol} that are obtained are different for two different firing temperatures.

A small but consistent difference may be seen in figure 3 between the B and C phases for the two most Eu-rich compositions. In both cases, $\chi_{mol}(B) < \chi_{mol}(C)$. Such a difference would be expected due to the different environments of the ions in the two structures, which result in different CFEs and exchange interactions.

Eu^{3+} ($4f^6$) is an anisotropic ion as a result of the orbital contribution to the J-value. Theoretical treatment of the anisotropic exchange between Eu^{3+} ions in the host Y_2O_3 has shown that at low concentrations the anisotropic exchange decreases [8, 22]. Our experimental data for $x \leqslant 0.2$ are consistent with this prediction. It was also shown that the isotropic exchange interaction in Eu_2O_3 decreases the χ-values, although the effect is small in comparison with the anisotropic one [22].

The increase in χ_{mol} for $x \leqslant 0.40$, obtained by Grill and Schieber [8] (figure 3), was ascribed to preferential occupation of 24d sites by magnetic Eu^{3+} ions. However, our results show no such increase (figure 3), and are consistent with Eu^{3+} occupying the 8b and 24d sites equally. Thus the random distribution obtained by x-ray diffraction is confirmed by magnetic susceptibility measurements.

4. Summary

The near-total cation disorder (random distribution) in C-$Y_{2-x}Eu_xO_3$ was determined from both x-ray and magnetic susceptibility measurements. The different firing temperatures do not influence the cationic distribution (figure 3). A preferential distribution in C-$Y_{2-x}Gd_xO_3$ [2] and C-$Y_{2-x}Eu_xO_3$ [8] was obtained in samples sintered under similar thermal conditions. The coprecipitation method leads to better solution of the two oxides and better sample homogeneity than the sintering method. Under similar sintering conditions C-$(Y, Gd)_2O_3$ shows different site preferences for the cations [2] whereas C-$(Y, Dy)_2O_3$ does not [3]. This change in behaviour can be attributed to the different sizes of the RE ions.

Acknowledgments

The authors thank Professor Lj Karanović and Mrs I Petrović-Prelević for help during the x-ray diffraction experiment.

References

[1] Marezio M 1966 *Acta Crystallogr.* **20** 723
[2] Mitric M, Onnerud P, Rodic D, Tellgren R, Szytula A and Napijalo M 1993 *J. Phys. Chem. Solids* **54** 967
[3] Antic B, Onnerud P, Rodic D and Tellgren R 1993 *Powder Diffract.* **8** 216
[4] Antic B, Mitric M and Rodic D 1995 *J. Magn. Magn. Mater.* **145** 349
[5] Beljaev R A 1974 *Svoistva Okislov Evropiya* (Moskva: Atomizdat) pp 13–8 and references therein
[6] Roth R S and Schneider S J 1960 *J. Res. NBS* A **64** 309

[7] Hoekstra H R 1966 *Inorg. Chem.* **5** 754
[8] Grill A and Schieber M 1970 *Phys. Rev.* B **1** 2241
[9] Kern S and Kostelecky R 1971 *J. Appl. Phys.* **42** 1773
[10] Borovik-Romanov A S and Kreines H M 1955 *Zh. Eksp. Teor. Fiz.* **6** 790
[11] *International Tables for X-ray Crystallography* 1974 vol IV (Birmingham: Kynoch) p 100
[12] Hovestreydt E 1983 *Acta Crystallogr.* A **39** 268
[13] Shannon R D and Prewitt C T 1969 *Acta Crystallogr.* B **25** 925
[14] Robinson K, Gibbs V G and Ribbe P H 1972 *Science* **172** 567
[15] Cromer D T 1957 *J. Phys. Chem.* **61** 753
[16] Yakel H L 1979 *Acta Crystallogr.* B **35** 564
[17] Landau D L and Lifshitz M E 1976 *Statisticheskaya Fizika* (Moskva: Nauka) pp 539–40
[18] Napijalo M 1972 *Savremena Istaživanja u Fizici II* ed B Dragović (Beograd: Naučna Knjiga) p 228
[19] Van Vleck J H 1932 *The Theory of Electric and Magnetic Susceptibilities* (London: Oxford University Press) p 245
[20] Arajs S and Colvin R V 1964 *J. Appl. Phys.* **35** 1181 and references therein
[21] Judd B R 1956 *Proc. Phys. Soc.* A **69** 157
[22] Huang N L and Van Vleck J H 1969 *J. Appl. Phys.* **40** 1145